Applied Physics Letters

Impact of N-plasma and Ga-irradiation on MoS_2 layer in molecular beam epitaxy

Cite as: Appl. Phys. Lett. **110**, 012101 (2017); https://doi.org/10.1063/1.4973371
Submitted: 30 September 2016 . Accepted: 13 December 2016 . Published Online: 03 January 2017

Pawan Mishra, Malleswararao Tangi, Tien Khee Ng, Mohamed Nejib Hedhili, Dalaver H. Anjum, Mohd Sharizal Alias, Chien-Chih Tseng, Lain-Jong Li, and Boon S. Ooi

AIP Publishing

Impact of N-plasma and Ga-irradiation on MoS_2 layer in molecular beam epitaxy

Pawan Mishra,[1] Malleswararao Tangi,[1] Tien Khee Ng,[1] Mohamed Nejib Hedhili,[2] Dalaver H. Anjum,[2] Mohd Sharizal Alias,[1] Chien-Chih Tseng,[3] Lain-Jong Li,[3] and Boon S. Ooi[1,a)]

[1]*Photonics Laboratory, Computer, Electrical, and Mathematical Sciences and Engineering (CEMSE), King Abdullah University of Science and Technology (KAUST), Thuwal 23955-6900, Saudi Arabia*
[2]*Imaging and Characterization Laboratory, King Abdullah University of Science and Technology (KAUST), Thuwal 23955-6900, Saudi Arabia*
[3]*Physical Science and Engineering Division, King Abdullah University of Science and Technology (KAUST), Thuwal 23955-6900, Saudi Arabia*

(Received 30 September 2016; accepted 13 December 2016; published online 3 January 2017)

Recent interest in two-dimensional materials has resulted in ultra-thin devices based on the transfer of transition metal dichalcogenides (TMDs) onto other TMDs or III-nitride materials. In this investigation, we realized p-type monolayer (ML) MoS_2, and intrinsic GaN/p-type MoS_2 heterojunction by the GaN overgrowth on ML-MoS_2/c-sapphire using the plasma-assisted molecular beam epitaxy. A systematic nitrogen plasma (N_2^*) and gallium (Ga) irradiation studies are employed to understand the individual effect on the doping levels of ML-MoS_2, which is evaluated by micro-Raman and high-resolution X-Ray photoelectron spectroscopy (HRXPS) measurements. With both methods, p-type doping was attained and was verified by softening and strengthening of characteristics phonon modes E^1_{2g} and A_{1g} from Raman spectroscopy. With adequate N_2^*-irradiation (3 min), respective shift of 1.79 cm^{-1} for A_{1g} and 1.11 cm^{-1} for E^1_{2g} are obtained while short term Ga-irradiated (30 s) exhibits the shift of 1.51 cm^{-1} for A_{1g} and 0.93 cm^{-1} for E^1_{2g}. Moreover, in HRXPS valence band spectra analysis, the position of valence band maximum measured with respect to the Fermi level is determined to evaluate the type of doping levels in ML-MoS_2. The observed values of valance band maximum are reduced to 0.5, and 0.2 eV from the intrinsic value of ≈1.0 eV for N_2^*- and Ga-irradiated MoS_2 layers, which confirms the p-type doping of ML-MoS_2. Further p-type doping is verified by Hall effect measurements. Thus, by GaN overgrowth, we attained the building block of intrinsic GaN/p-type MoS_2 heterojunction. Through this work, we have provided the platform for the realization of dissimilar heterostructure via monolithic approach.
[http://dx.doi.org/10.1063/1.4973371]

The recent investigations reveal that the dissimilar heterojunctions formed by transition metal dichalcogenides (TMDs) and III-nitrides provide the route for novel devices in the area of optoelectronic, electronics, and water splitting applications.[1–4] In addition, 2D materials such as graphene, boron nitride nanosheets, and layered transition metal dichalcogenides (TMDs) were investigated as potential buffer layers for the epitaxial growth of III–V semiconductors on foreign substrates.[5–8] The use of TMDs, in particular, layered-MoS_2 as a buffer layer attracts the potential interest of researchers to address the issues such as large lattice and thermal expansion mismatch for the growth of GaN.[9,10] Recently, GaN epitaxy on layered-MoS_2 flakes was demonstrated using high temperature (∼1000 °C) growth process of metal-organic chemical vapor deposition (MOCVD).[5]

In contrast to the MOCVD process, molecular beam epitaxy (MBE) has the advantage of low growth temperature and ultra-high vacuum (UHV) with a low partial pressure of oxygen (∼10^{-11} Torr). Yamada *et al.* demonstrated GaN epitaxy using MBE on bulk and layered-MoS_2.[11,12] In their work, they investigated the effect of nitrogen plasma (N_2^*) and Ga-irradiation on the surface morphology of overgrown GaN. However, the effect of N_2^*- and Ga-irradiation on the 2D layered-MoS_2 in high to ultra-high vacuum (UHV) environment has not been explored. Focusing on MoS_2, the tunability of doping,[13–17] optical,[18–20] and structural,[21] properties of the layered-MoS_2 has been reported by employing the plasma (O_2^* or N_2^*) irradiation. However, in most of these studies, ∼150 Torr of the background utilized during plasma irradiation, whereas in plasma-assisted MBE (PAMBE), low background ∼10^{-6} Torr can be used for tuning the properties of layered-MoS_2. Here, we present the demonstration of p-type monolayer (ML) MoS_2, by N_2^*- and Ga-irradiation under UHV conditions using PAMBE, and subsequently demonstrated the intrinsic GaN/p-type MoS_2 heterojunction by GaN overgrowth.

We deposited layered-MoS_2 on the c-sapphire substrates using CVD, details published elsewhere.[22] The N_2^*- and Ga-irradiation were performed using VEECO GEN930 PAMBE system at a substrate temperature of 450 °C. Active nitrogen species (N_2^*) were provided by using a Veeco Uni-Bub radio

a)Author to whom correspondence should be addressed. Electronic mail: boon.ooi@kaust.edu.sa

frequency plasma N_2 source supplied through inert gas purifier fed with high purity N_2 gas (99.9999%). N_2 plasma conditions, i.e., RF power 300 W, N_2 flow rate 1 sccm were used. Ga was evaporated by standard dual filament Knudsen cell with beam equivalent pressure (BEP) value of 6×10^{-8} Torr. The realization of p-type MoS_2 through N_2^*- and Ga-irradiation were confirmed by using Raman spectroscopy and high-resolution X-Ray photoelectron spectroscopy (HRXPS) analyses. For analyzing the optical quality of ML-MoS_2 samples post MBE processes, micro-photoluminescence (PL) spectroscopy was used. Further, GaN growth on ML-MoS_2\sapphire was implemented in PAMBE by using two step 450 °C\700 °C growth temperatures. Further, aberration corrected high angle annular dark field (HAADF) high-resolution scanning transmission electron microscopy (HR-STEM) cross-section analysis was used to characterize GaN/MoS_2 interface. Cross-section specimen preparation method and operational details for HRSTEM are described in our previous work.[23] For micro-PL and micro-Raman spectroscopy, we used 473 and 325 nm laser sources equipped in Horiba Aramis system. The high-resolution X-Ray photoelectron spectroscopy (HRXPS) studies were carried out with a Kratos Axis Ultra DLD spectrometer equipped with a monochromatic Al Kα x-ray source ($h\nu = 1486.6$ eV) operating at 150 W, a multichannel plate, and a delay line detector under a vacuum of 7.5×10^{-10} Torr. The samples were mounted in a floating mode in order to avoid differential charging. Binding energies were referenced to the C 1s binding energy of adventitious carbon contamination which was taken to be 284.8 eV. Single magnetic field Hall effect measurement system was used to determine sheet carrier concentration of samples at Room Temperature (RT).

Fig. 1(a) shows the Raman spectrum of the pristine-MoS_2 and N_2^*-irradiated layered-MoS_2 samples. The pristine-MoS_2 exhibits characteristic phonon modes, i.e., in-plane E^1_{2g} and out-of-plane A_{1g} modes at ~385.3 cm^{-1} and ~405 cm^{-1}, respectively, which stem from the monolayer of pristine-MoS_2.[22,24–26] Relative to pristine ML-MoS_2, the shift of 1.79 cm^{-1} (for A_{1g}) and 1.11 cm^{-1} (for E^1_{2g}) towards higher and lower wavenumber values, respectively, obtained for the 3 min N_2^*-irradiated ML-MoS_2. Such relative shift of phonon modes in the opposite direction has been predicted to be caused by p-type doping in ML-MoS_2.[26] As pristine ML-MoS_2 prone to have S vacancies, hence the incorporation of N atoms is favorable during N_2^*-irradiation.[26,27] Therefore, enhancement of compressive strain with increasing N incorporation in ML-MoS_2 occurs, due to smaller atomic radii of N atoms as compared to that of sulfur (S) atoms, and hence promoting softening of E^1_{2g} phonon mode.[17,28] On the other hand, for n-type doping, softening of A_{1g} phonon mode, thus, shifts towards lower wavenumber has been reported.[29] Further enhancement in carrier concentration has been identified by the increase in the peak intensities ratio, i.e., $I(A_{1g})/I(E^1_{2g})$ (from 2.11 to 2.24) for N_2^*-irradiated samples as shown in Fig. 1(b). For mulilayered-MoS_2 and ML-MoS_2, such increase in the $I(A_{1g})/I(E^1_{2g})$ value has been attributed to the increasing the carrier density for p- as well as n-type of doping.[15,26,30] Such increase in the intensity ratio is due to the suppressed in-plane movement of the Mo–S atom and thus suppressing E^1_{2g} under enhanced compressive strain due to the N incorporation.[31] However, with increasing N_2^*-irradiation time, FWHM of E^1_{2g} also increases from 5.63 (for pristine-MoS_2) to 11.09 (for 3 min N_2^*-irradiation) as shown in Fig. 1(b). Such increase in the FWHM points towards the increase in the doping level as well as defects generation.

Figs. 2(a)–2(c) show the Mo 3d, Mo $3p_{3/2}$/N 1s, and S 2p XPS spectra for the pristine and N_2^*-irradiated (for 1 and 3 min) ML-MoS_2. Mo $3d_{5/2}$, Mo $3p_{3/2}$, and S $2p_{3/2}$ peaks show shifts toward lower binding energies for N_2^*-irradiated ML-MoS_2 samples. In particular, Mo $3d_{5/2}$ peak for pristine ML-MoS_2 obtained at 229.8 eV, after the N_2^*-irradiation for 3 min shift of 0.2 eV towards lower binding energy is obtained. In addition, the Mo$3p_{3/2}$/N 1s region shows the existence of N 1s peak at binding energy ~398.7 eV after N_2^*-irradiation of ML-MoS_2 confirming the formation of N-Mo bonds[14,15,17] as shown in Fig. 2(b) and thus confirming p-type doping. From the valence band spectra (Figs. 2(d)–2(f)), we obtained valance band maximum (VBM) of pristine ML-MoS_2 is 1 eV, which is in consistent with the previous value in literature.[4,32] For N_2^*-irradiated MoS_2 samples for 1 min (3 min), the binding energy of VBM is 0.9 (0.5) eV.

It is found that the VBM decreases with increasing N_2^*-irradiation time and hence confirming the enhancement of p-type doping in layered-MoS_2 as predicted by the analysis of Raman spectroscopy results.[33] As CVD grown pristine-MoS_2 has the n-type semiconducting behavior because of S vacancies and thus realization of p-type doping is quite challenging especially in the case of mono or bilayer MoS_2. Using our approach of N_2^*-irradiation, we demonstrated a reduction in E_V-E_F, which shows a change in polarity of the carriers. Further increment in the carriers without significant

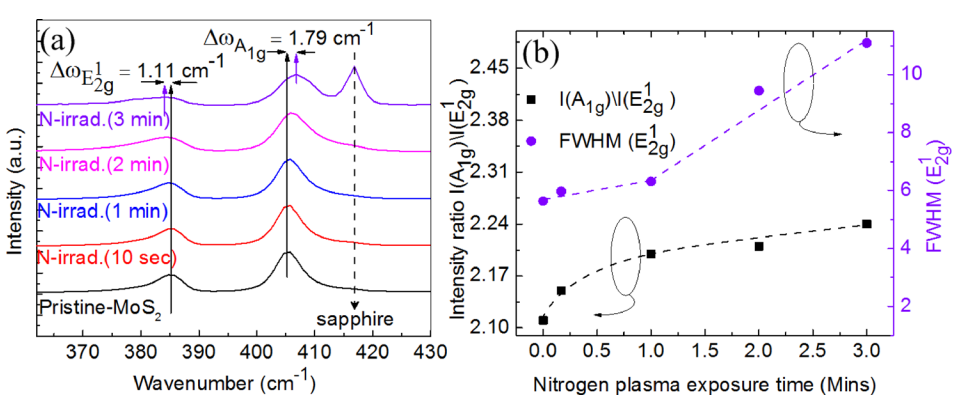

FIG. 1. (a) Raman spectroscopy of pristine and N_2^*-irradiated ML-MoS_2. (b) Intensity ratio of characteristic phonon modes, i.e., $I(A_{1g})/I(E^1_{2g})$ and FWHM of E^1_{2g} versus plasma irradiation time.

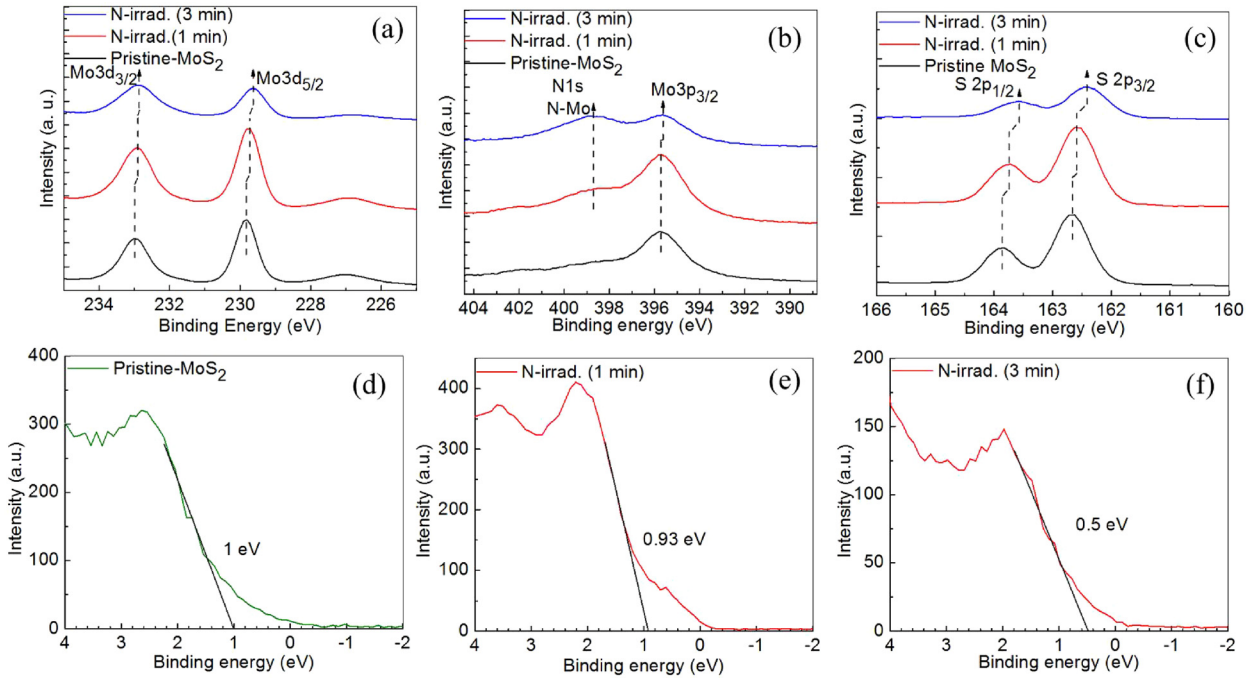

FIG. 2. (a) Mo 3d, (b) Mo $3p_{3/2}$/N 1s, and (c) S 2p HRXPS spectra of pristine-MoS_2 and plasma treated (for 1 min and 3 min) layered-MoS_2. (d) The valence-band spectrum for pristine-MoS_2 and N_2^*-irradiated ML-MoS_2 samples for (e) 1 min and (f) 3 min.

physical damage to the layered-MoS_2 will remain a process optimization challenge, which may be addressed by adopting the low brightness mode of nitrogen plasma irradiation for a longer time.

Further, we investigated the effect of Ga-irradiation on ML-MoS_2. Fig. 3(a) shows the Raman spectroscopy of pristine-, Ga-irradiated, and 2-step, i.e., Ga-irradiation for 30 s (step 1)/N_2^*-irradiation for 1 min (step 2) treated ML-MoS_2 samples. Similar to N_2^*-irradiated MoS_2, softening in E^1_{2g} phonon mode by 0.93 cm^{-1} (2.83 cm^{-1}) is obtained for Ga-irradiated (2-step treated) MoS_2 sample as shown in Fig. 3(a). In addition, uplift in the $I(A_{1g})/I(E^1_{2g})$ values, i.e., 2.46 and 2.31, is obtained for Ga-irradiated (30 s) and 2-step treated sample, respectively, as compared to that of 2.11 for pristine ML-MoS_2. Also, increase in FWHM as shown in Fig. 3(b) after Ga-irradiation shows the enhancement in doping as well as possible degradation of ML-MoS_2.

Fig. 3(c) shows the room temperature PL results of pristine, N_2^*-, and Ga-irradiated samples. PL intensity reduction with both methods has been observed which indicates

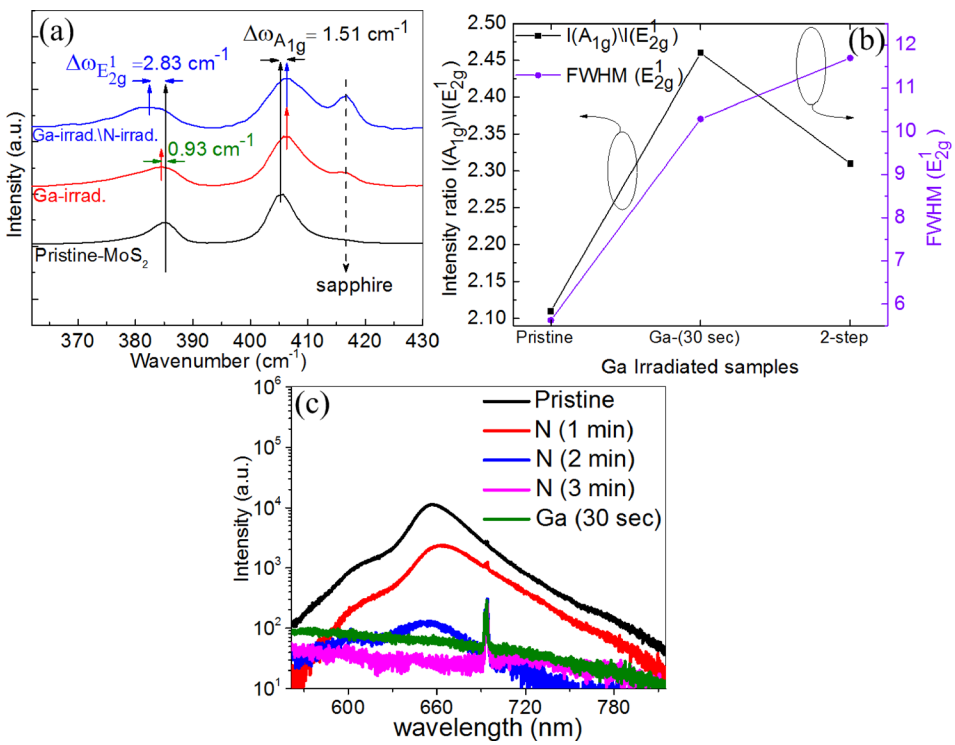

FIG. 3. (a) Raman spectroscopy of pristine-, Ga irradiated, and 2-step, i.e., Ga-irradiation (step 1)\N_2^*-irradiation (step 2) treated ML-MoS_2 samples. (b) Intensity ratio of characteristic phonon modes, i.e., $I(A_{1g})/I(E^1_{2g})$ and FWHM of E^1_{2g} for Ga-irradiated MoS_2 samples. (c) Photoluminescence of N_2^*- and Ga-irradiated MoS_2 samples at room temperature.

structural degradation of MoS_2 layers. However, softening of E^1_{2g} and enhancement of $I(A_{1g})/I(E^1_{2g})$ indicates towards p-type doping of ML-MoS_2 after N^*_2- and Ga-irradiation.

Fig. 4(a) shows Mo $3d_{5/2}$ peaks shifted toward lower binding energies for Ga-irradiated samples relative to that of pristine ML-MoS_2. Fig. 4(b) shows Ga 2p for pristine ML-MoS_2 and Ga irradiated sample. The existence of Ga $2p_{1/2}$ and Ga $2p_{3/2}$ core levels at 1144 and 1117 eV, respectively, reveals the incorporation of Ga into MoS_2 post Ga-irradiation. It is important to point out that the short duration (30 s) and the use of low Ga flux beam equivalent pressure (BEP) of 6×10^{-8} Torr during Ga-irradiation ensured no deposition of Ga adlayers on layered-MoS_2. Moreover, for Ga-irradiated MoS_2 the reduced value of binding energy of VBM (0.2 eV) is obtained 0.2 as shown in Fig. 4(c), which has similar trend obtained for N^*_2-irradiated samples and hence confirming the realization of p-type ML-MoS_2.[17,34]

Such reduction in binding energy of VBM also confirms the absence of inelastic scattering of electrons at the surface of ML-MoS_2. In Ga-irradiated samples sulfur vacancies were occupied by Ga atoms and hence enabling the p-type behavior. Fig. 4(d) shows the energy band diagrams of pristine ML-MoS_2 and p-type ML-MoS_2 realized by N^*_2- and Ga-irradiation in MBE. The reported electronic bandgap of 2.15 eV for the ML-MoS_2 has been used in the energy band diagram.[32] For N^*_2- and Ga-irradiated MoS_2 samples, E_V–E_F is 0.5 eV and 0.2 eV, respectively. These values are comparable with that of other p-type TMDs and Si.[33,38] Further, the polarity change of carriers for pristine and treated samples were verified by Van der-Pauw Hall effect measurements having the sheet hole carrier concentration in the range of 2.64×10^{12} to 5.74×10^{13} cm^{-2}, which is consistent with the literature as shown in Figs. 4(e) and 4(f).[15,34–37]

Subsequently, GaN/MoS_2 heterojunction was realized by an overgrowth of GaN on ML-MoS_2 using PAMBE, and retainability of MoS_2 layer after MBE processes was investigated. Fig. 5(a) shows a cross-section image of GaN/ML-MoS_2/c-sapphire using HAADF-HRSTEM. The interface between MoS_2 and GaN is observed to be not as sharp as the interface between sapphire and MoS_2 as described by the elemental profiles and mapping in Fig. 5(b) and respective inset. Observed interdiffusion in compositional mapping at MoS_2 and GaN interface attributed to the interaction of Ga and N^*_2 with layered-MoS_2, which validates the tuning of aforementioned doping properties of layered-MoS_2 in MBE.

In conclusion, we demonstrated the p-type doping in the ML-MoS_2 in ultra-high vacuum MBE environment via N^*_2- and Ga-irradiation. Nondestructive Raman spectroscopy

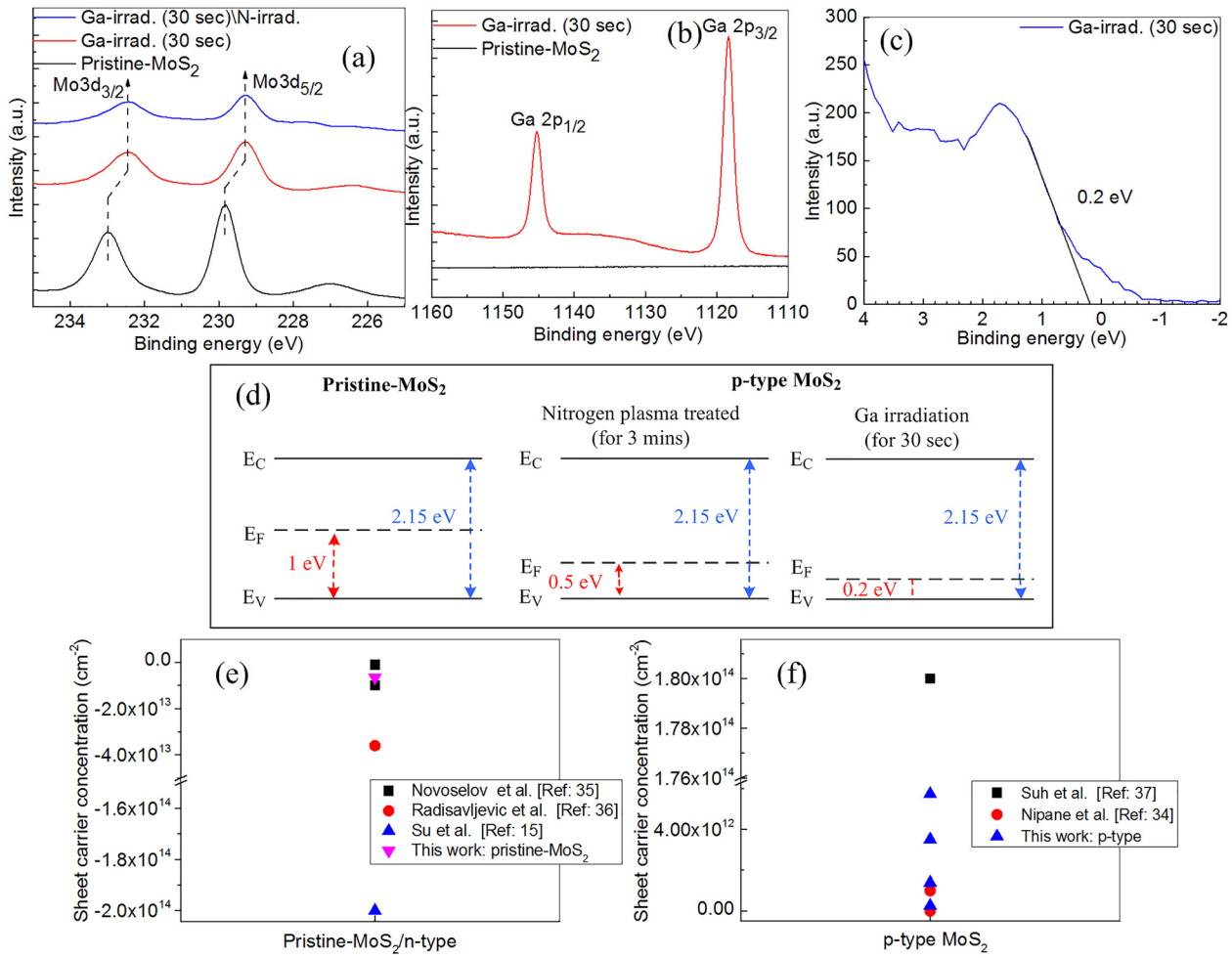

FIG. 4. (a) Mo 3d HRXPS spectra of pristine-, Ga-irradiated, and 2-step, i.e., Ga-irradiation (step 1)\N^*_2-irradiation (step 2), treated ML-MoS_2 samples. (b) HRXPS spectra of Ga 2p core level on Ga-irradiated and pristine-MoS_2 samples. (c) The valence-band spectrum of Ga-irradiated ML-MoS_2. (d) Energy band diagrams of pristine ML-MoS_2 and p-type ML-MoS_2 realized by N^*_2- and Ga-irradiation. (e) Sheet carrier concentrations (cm^{-2}) for pristine-MoS_2 and (f) realized p-type MoS_2 layers and their comparison with the values taken from the existing literature.[15,34–37]

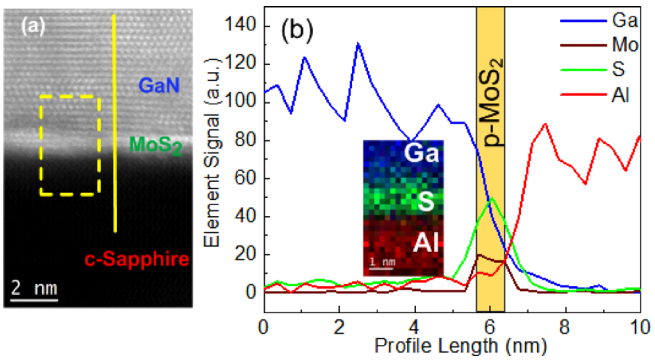

FIG. 5. (a) HAADF-HRSTEM. (b) electron energy loss spectroscopy (EELS) line profiles for the GaN/p-MoS_2/sapphire interfaces with energy dispersive spectroscopy (EDS) compositional mapping as an inset corresponding to the highlighted part in the HAADF-HRSTEM image.

results revealed softening of E^1_{2g} and uplift of $I(A_{1g})/I(E^1_{2g})$ in irradiated samples and thus confirming p-type doping and increment of carrier concentration. The reduced $(E_F\text{-}E_V)$ values, i.e., 0.5 eV (0.2 eV) obtained in the HRXPS analysis for N^*_2- (Ga-) irradiated sample, reveal p-type doping. Further, change of carrier polarity was observed in Hall effect measurements. HAADF-STEM results revealed the retainability of ML-MoS_2 even after MBE processes and showed the interaction between Ga and N atoms/active species with ML-MoS_2. MBE based GaN on MoS_2 was demonstrated to realize GaN/p-MoS_2 heterojunction. Such demonstrations pave the way for the realization of multiple quantum wells constituting III-nitrides as a quantum barrier and TMDs as a quantum well layer for application in optoelectronic and electronics devices.

This publication is based upon the work supported by the King Abdulaziz City for Science and Technology (KACST), Grant No. KACST TIC R2-FP-008, and the King Abdullah University of Science and Technology (KAUST) baseline funding BAS/1/1614-01-01.

[1]H. Jeong, S. Bang, H. M. Oh, H. J. Jeong, S. J. An, G. H. Han, H. Kim, K. K. Kim, J. C. Park, Y. H. Lee, G. Lerondel, and M. S. Jeong, ACS Nano **9**(10), 10032–10038 (2015).
[2]J. M. Liao, B. S. Sa, J. Zhou, R. Ahuja, and Z. M. Sun, J. Phys. Chem. C **118**(31), 17594–17599 (2014).
[3]E. W. Lee, C. H. Lee, P. K. Paul, L. Ma, W. D. McCulloch, S. Krishnamoorthy, Y. Wu, A. R. Arehart, and S. Rajan, Appl. Phys. Lett. **107**(10), 103505 (2015).
[4]M. Tangi, P. Mishra, T. K. Ng, M. N. Hedhili, B. Janjua, M. S. Alias, D. H. Anjum, C.-C. Tseng, Y. Shi, H. J. Joyce, L.-J. Li, and B. S. Ooi, Appl. Phys. Lett. **109**(3), 032104 (2016).
[5]P. Gupta, A. A. Rahman, S. Subramanian, S. Gupta, A. Thamizhavel, T. Orlova, S. Rouvimov, S. Vishwanath, V. Protasenko, M. R. Laskar, H. G. Xing, D. Jena, and A. Bhattacharya, Sci. Rep. **6**, 23708 (2016).
[6]Y. Alaskar, S. Arafin, D. Wickramaratne, M. A. Zurbuchen, L. He, J. McKay, Q. Y. Lin, M. S. Goorsky, R. K. Lake, and K. L. Wang, Adv. Funct. Mater. **24**(42), 6629–6638 (2014).
[7]T. Araki, S. Uchimura, J. Sakaguchi, Y. Nanishi, T. Fujishima, A. Hsu, K. K. Kim, T. Palacios, A. Pesquera, A. Centeno, and A. Zurutuza, Appl. Phys. Express **7**(7), 071001 (2014).
[8]L. Zhang, X. L. Li, Y. L. Shao, J. X. Yu, Y. Z. Wu, X. P. Hao, Z. M. Yin, Y. B. Dai, Y. Tian, Q. Huo, Y. A. Shen, Z. Hua, and B. G. Zhang, ACS Appl. Mater. Interfaces **7**(8), 4504–4510 (2015).
[9]L. Zhang, K. Cheng, S. Degroote, M. Leys, M. Germain, and G. Borghs, J. Appl. Phys. **108**(7), 073522 (2010).
[10]S. A. Kukushkin, A. V. Osipov, V. N. Bessolov, B. K. Medvedev, V. K. Nevolin, and K. A. Tcarik, Rev. Adv. Mater. Sci. **17**, 1 (2008).
[11]A. Yamada, K. P. Ho, T. Akaogi, T. Maruyama, and K. Akimoto, J. Cryst. Growth **201**, 332–335 (1999).
[12]A. Yamada, K. P. Ho, T. Maruyama, and K. Akimoto, Appl. Phys. A-Mater. **69**(1), 89–92 (1999).
[13]M. Chen, H. Nam, S. Wi, L. Ji, X. Ren, L. Bian, S. Lu, and X. Liang, Appl. Phys. Lett. **103**(14), 142110 (2013).
[14]S. Qin, W. W. Lei, D. Liu, and Y. Chen, Sci. Rep. **4**(1–5), 7582 (2014).
[15]T.-H. Su and Y.-J. Lin, Appl. Phys. Lett. **108**(3), 033103 (2016).
[16]M. R. Islam, N. Kang, U. Bhanu, H. P. Paudel, M. Erementchouk, L. Tetard, M. N. Leuenberger, and S. I. Khondaker, Nanoscale **6**(17), 10033–10039 (2014).
[17]A. Azcatl, X. Qin, A. Prakash, C. Zhang, L. Cheng, Q. Wang, N. Lu, M. J. Kim, J. Kim, K. Cho, R. Addou, C. L. Hinkle, J. Appenzeller, and R. M. Wallace, Nano Lett. **16**(9), 5437–5443 (2016).
[18]N. R. Kang, H. P. Paudel, M. N. Leuenberger, L. Tetard, and S. I. Khondaker, J. Phys. Chem. C **118**(36), 21258–21263 (2014).
[19]R. Dhall, M. R. Neupane, D. Wickramaratne, M. Mecklenburg, Z. Li, C. Moore, R. K. Lake, and S. Cronin, Adv. Mater. **27**(9), 1573–1578 (2015).
[20]M. S. Kim, G. Nam, S. Park, H. Kim, G. H. Han, J. Lee, K. P. Dhakal, J. Y. Leem, Y. H. Lee, and J. Kim, Thin Solid Films **590**, 318–323 (2015).
[21]G. L. Ye, Y. J. Gong, J. H. Lin, B. Li, Y. M. He, S. T. Pantelides, W. Zhou, R. Vajtai, and P. M. Ajayan, Nano Lett. **16**(2), 1097–1103 (2016).
[22]Y. H. Lee, X. Q. Zhang, W. J. Zhang, M. T. Chang, C. T. Lin, K. D. Chang, Y. C. Yu, J. T. W. Wang, C. S. Chang, L. J. Li, and T. W. Lin, Adv. Mater. **24**(17), 2320–2325 (2012).
[23]P. Mishra, B. Janjua, T. K. Ng, D. H. Anjum, R. T. Elafandy, A. Prabaswara, C. Shen, A. Salhi, A. Y. Alyamani, M. M. El-Desouki, and B. S. Ooi, Opt. Mater. Express **6**(6), 2052–2062 (2016).
[24]R. S. Yan, J. R. Simpson, S. Bertolazzi, J. Brivio, M. Watson, X. F. Wu, A. Kis, T. F. Luo, A. R. H. Walker, and H. G. Xing, ACS Nano **8**(1), 986–993 (2014).
[25]N. A. Lanzillo, A. G. Birdwell, M. Amani, F. J. Crowne, P. B. Shah, S. Najmaei, Z. Liu, P. M. Ajayan, J. Lou, M. Dubey, S. K. Nayak, and T. P. O'Regan, Appl. Phys. Lett. **103**(9), 093102 (2013).
[26]W. Zhou, X. L. Zou, S. Najmaei, Z. Liu, Y. M. Shi, J. Kong, J. Lou, P. M. Ajayan, B. I. Yakobson, and J. C. Idrobo, Nano Lett. **13**(6), 2615–2622 (2013).
[27]L. M. Yang, K. Majumdar, H. Liu, Y. C. Du, H. Wu, M. Hatzistergos, P. Y. Hung, R. Tieckelmann, W. Tsai, C. Hobbs, and P. D. Ye, Nano Lett. **14**(11), 6275–6280 (2014).
[28]C. Rice, R. J. Young, R. Zan, U. Bangert, D. Wolverson, T. Georgiou, R. Jalil, and K. S. Novoselov, Phys. Rev. B **87**(8), 081307 (2013).
[29]B. Chakraborty, A. Bera, D. V. S. Muthu, S. Bhowmick, U. V. Waghmare, and A. K. Sood, Phys. Rev. B **85**(16), 161403 (2012).
[30]M. R. Laskar, D. N. Nath, L. Ma, E. W. Lee, C. H. Lee, T. Kent, Z. Yang, R. Mishra, M. A. Roldan, J.-C. Idrobo, S. T. Pantelides, S. J. Pennycook, R. C. Myers, Y. Wu, and S. Rajan, Appl. Phys. Lett. **104**(9), 092104 (2014).
[31]A. P. Nayak, T. Pandey, D. Voiry, J. Liu, S. T. Moran, A. Sharma, C. Tan, C. H. Chen, L. J. Li, M. Chhowalla, J. F. Lin, A. K. Singh, and D. Akinwande, Nano Lett. **15**(1), 346–353 (2015).
[32]M. H. Chiu, C. D. Zhang, H. W. Shiu, C. P. Chuu, C. H. Chen, C. Y. S. Chang, C. H. Chen, M. Y. Chou, C. K. Shih, and L. J. Li, Nat. Commun. **6**, 7666 (2015).
[33]C. H. Chen, C. L. Wu, J. Pu, M. H. Chiu, P. Kumar, T. Takenobu, and L. J. Li, 2d Mater. **1**(3), 034001 (2014).
[34]A. Nipane, D. Karmakar, N. Kaushik, S. Karande, and S. Lodha, ACS Nano **10**(2), 2128–2137 (2016).
[35]K. S. Novoselov, D. Jiang, F. Schedin, T. J. Booth, V. V. Khotkevich, S. V. Morozov, and A. K. Geim, Proc. Natl. Acad. Sci. U. S. A. **102**(30), 10451–10453 (2005).
[36]B. Radisavljevic, A. Radenovic, J. Brivio, V. Giacometti, and A. Kis, Nat. Nanotechnol. **6**(3), 147–150 (2011).
[37]J. Suh, T. E. Park, D. Y. Lin, D. Y. Fu, J. Park, H. J. Jung, Y. B. Chen, C. Ko, C. Jang, Y. H. Sun, R. Sinclair, J. Chang, S. Tongay, and J. Q. Wu, Nano Lett. **14**(12), 6976–6982 (2014).
[38]C. C. Hu, *Modern Semiconductor Devices for Integrated Circuits* (Prentice Hall, 2011).